

the reactions reported herein.

Use of Cross-Reaction Rate Constants for Probing Steric (Nonadiabatic) Effects in Electron-Transfer Reactions. In its complete form, Marcus' theory considers the possibility of nonadiabatic effects through a prefactor, p , in the expression for the rate constant. This prefactor is essentially a transmission coefficient. Equation 1 assumes an adiabatic transfer in which p is unity, whereas the more complete expression is

$$k_{12} = p_{12} Z_{12} \exp(-\Delta G^*_{12}/RT) \quad (16)$$

Sutin has pointed out that the use of eq 14, the correlation equation, will fail to identify nonunity prefactors as long as

$$p_{12} = (p_{11} p_{22})^{1/2} \quad (17)$$

where p_{11} and p_{22} express the nonadiabaticity in the appropriate self-exchange processes and if K_{12} is not large.⁸ This result is fortuitous in that it aids in the application of the correlation equation, but the apparent success of eq 14 and 15 may be incorrectly used to justify the notion that most outer-sphere electron transfers are adiabatic.

The calculations that were used to construct Figures 2-5 were not susceptible to the problem discussed above because we used calculated as opposed to measured self-exchange rate constants for the sterically hindered complexes. The observed k_{11} values for these couples could be significantly less than the calculated values ($p_{11} < 1$), and if experimental values were known, the agreement between calculated and observed cross-reaction rate constants might be much better than it is.

Conclusions

Three series of structurally related redox couples based on $\text{Ru}(\text{NH}_3)_5(\text{py})^{3+,2+}$, $\text{Co}(\text{phen})_3^{3+,2+}$, and $\text{Cu}(\text{H}_2\text{G}_3)^{0,-}$ have been prepared. In each series, the donor atoms and coordination geometry remain the same, but organic substituents of

increasing size are introduced on the periphery of the ligands. The electronic spectra and electrochemical properties of the complexes indicate that organic substituents do not produce dramatic or unpredictable changes in these physical properties.

Rate constants for outer-sphere electron-transfer reactions between the $\text{Ru}(\text{III})$ and $\text{Co}(\text{II})$ and the $\text{Cu}(\text{III})$ and $\text{Co}(\text{II})$ complexes have been measured. The rate constants for both sets of reactions have the same dependence on driving force, and this dependence is close to the prediction of Marcus' theory. When the observed rate constants are compared to calculated values, the rates of reactions involving the complexes with the larger organic substituents appear to be attenuated, possibly due to nonadiabaticity. These trends are especially evident for the $\text{Ru}(\text{III}) + \text{Co}(\text{II})$ reactions, while the trends for the $\text{Cu}(\text{III}) + \text{Co}(\text{II})$ reactions are less straightforward.

In order to understand these steric effects it will be necessary to (i) synthesize additional ligands with even larger organic substituents, (ii) measure self-exchange rate constants for some of the complexes with large organic substituents, and (iii) determine activation entropies for some of the cross-reactions. These experiments are in progress in our laboratories.

Acknowledgment. This material is based upon work supported by the National Science Foundation under Grant 8204000. Acknowledgment is made to the donors of the Petroleum Research Fund, administered by the American Chemical Society, and to the Research Corp. for partial support of this research. The authors thank Arlene W. Hamburg for advice on synthesis and a sample of the peptide Aib₃ and Dale W. Margerum for useful discussions and a copy of his stopped-flow acquisition and analysis program.

Registry No. I^{2+} , 21360-09-8; II^{2+} , 19482-30-5; III^{2+} , 88326-60-7; IV^{2+} , 16788-34-4; V^{2+} , 47872-45-7; VI^{2+} , 88326-61-8; VII , 62801-36-9; VIII , 69042-71-3; IX , 69990-31-4; X , 88326-62-9.

Contribution from the Department of Chemistry, Purdue University, West Lafayette, Indiana 47907

Gas-Phase Reactions of Co^+ and Rh^+ with Toluene, Cycloheptatriene, and Norbornadiene

D. B. JACOBSON, G. D. BYRD, and B. S. FREISER*

Received December 10, 1982

The gas-phase reactions of toluene, cycloheptatriene, and norbornadiene with Co^+ and Rh^+ are described. The dominant process for Rh^+ is dehydrogenation, generating a RhC_7H_6^+ complex. These RhC_7H_6^+ ions decompose, yielding RhC^+ (benzene loss), presumably through the intermediacy of a carbide-benzene complex. Rh^+ dehydrogenates toluene- $\alpha,\alpha,\alpha\text{-d}_3$ to eliminate both D_2 (70%) and HD (30%). Cobalt ions react quite differently with no CoC_7H_6^+ or CoC^+ observed. Both Co^+ and Rh^+ abstract hydride from cycloheptatriene, implying $D^\circ(\text{Co-H}) > 38$ kcal/mol and $D^\circ(\text{Rh-H}) > 47$ kcal/mol. The gas-phase chemistry of Rh^+ is similar to the chemistry observed on metal surfaces for cycloheptatriene and norbornadiene.

Introduction

The chemistry of various hydrocarbons on metal surfaces has been intensely studied with regard to catalytic processes.¹ In particular, the surface chemistry of several cyclic olefins and polyenes has been the focus of recent investigations.²⁻⁷ An intriguing observation in these studies is the surface-mediated

conversions of cycloheptatriene and norbornadiene to benzene.⁶ The processes occurring on these metal surfaces are ill-defined. Concurrently, the study of gas-phase reactions of transition-metal ions with organic species has been rapidly expanding and is aimed at understanding the metal-organic interaction on a fundamental level.⁸⁻¹⁰ Most of these studies have cen-

- (1) Thomson, S. J. *Spec. Period. Rep.: Catalysis* 1977, 1.
- (2) Tsai, M.-C.; Friend, C. M.; Muettterties, E. L. *J. Am. Chem. Soc.* 1982, 104, 2539.
- (3) Tsai, M.-C.; Muettterties, E. L. *J. Phys. Chem.* 1982, 86, 5067.
- (4) Tsai, M.-C.; Muettterties, E. L. *J. Am. Chem. Soc.* 1982, 104, 2534.
- (5) Friend, C. M.; Muettterties, E. L. *J. Am. Chem. Soc.* 1981, 103, 773.
- (6) Tsai, M.-C.; Stein, J.; Freind, C. M.; Muettterties, E. L. *J. Am. Chem. Soc.* 1982, 104, 3533.
- (7) (a) Muettterties, E. L. In "Reactivity of Metal-Metal Bonds"; Chisholm, M. H., Ed.; American Chemical Society: Washington, DC, *ACS Symp. Ser. No. 155*, p 273. (b) Muettterties, E. L. *Chem. Soc. Rev.* 1982, 11, 283.

- (8) (a) Allison, J.; Ridge, D. P. *J. Organomet. Chem.* 1975, 99, C11-C14. (b) Allison, J.; Ridge, D. P. *J. Am. Chem. Soc.* 1979, 101, 4998. (c) Allison, J.; Freas, R. B.; Ridge, D. P. *Ibid.* 1979, 101, 1332.
- (9) (a) Armentrout, P. B.; Beauchamp, J. L. *J. Am. Chem. Soc.* 1981, 103, 784. (b) Armentrout, P. B.; Halle, L. F.; Beauchamp, J. L. *Ibid.* 1981, 103, 6624. (c) Armentrout, P. B.; Beauchamp, J. L. *Ibid.* 1981, 103, 6628. (d) Halle, L. F.; Armentrout, P. B.; Beauchamp, J. L. *Organometallics* 1982, 1, 984.
- (10) (a) Burnier, R. C.; Byrd, G. D.; Freiser, B. S. *J. Am. Chem. Soc.* 1981, 103, 4360. (b) Byrd, G. D.; Burnier, R. C.; Freiser, B. S. *Ibid.* 1982, 104, 3565. (c) Jacobson, D. B.; Freiser, B. S. *Ibid.* 1983, 105, 736. (d) Jacobson, D. B.; Freiser, B. S. *Ibid.* 1983, 105, 5197.

Table I. Product Distributions for Reactions of Co⁺ and Rh⁺ with Three C₇H₈ Isomers

isomer	M = Co			M = Rh		
	neutral	ion	rel %	neutral	ion	rel %
toluene		CoC ₇ H ₈	100	H ₂	RhC ₇ H ₆	100
cycloheptatriene	H·	CoC ₇ H ₇	4	H ₂	RhC ₇ H ₆	44
	CH ₂	CoC ₆ H ₆	6	CH ₂	RhC ₆ H ₆	2
	C ₂ H ₂	CoC ₅ H ₆	34	C ₂ H ₂	RhC ₅ H ₆	6
	C ₅ H ₆	CoC ₂ H ₂	1	C ₆ H ₆	RhCH ₂	7
	C ₆ H ₆	CoCH ₂	39	C ₆ H ₆ , H ₂ ^a	RhC	30
	Co	C ₇ H ₈	3	RhH	C ₇ H ₇	11
	CoH	C ₇ H ₇	13			
norbornadiene	CH ₂	CoC ₆ H ₆	1	H ₂	RhC ₇ H ₆	16
	C ₂ H ₂	CoC ₅ H ₆	82	CH ₂	RhC ₆ H ₆	2
	C ₅ H ₆	CoC ₂ H ₂	12	C ₂ H ₂ ^b	RhC ₅ H ₆	25
	C ₆ H ₆	CoCH ₂	5	C ₂ H ₃ ^b	RhC ₅ H ₅	5
				C ₆ H ₆ , H ₂ ^a	RhCH ₂	10
				RhC	42	

^a This loss may be either C₆H₈ or H₂ and C₆H₆ as listed here; see text for details. ^b This loss may be either C₂H₃· as listed or C₂H₂ and H·; see text for explanation.

tered on the reactions of monatomic metal cations with saturated organic molecules.

In this study we apply Fourier transform mass spectrometry (FTMS)¹¹ to study the reactions of laser-desorbed Co⁺ and Rh⁺ with the C₇H₈ isomers toluene, cycloheptatriene, and norbornadiene. The results for both metal ions are compared and contrasted. In addition, the gas-phase results are compared to the metal-surface chemistry for these three C₇H₈ isomers.

Experimental Section

All experiments were performed on a prototype Nicolet FTMS-1000 Fourier transform mass spectrometer previously described in detail¹² and equipped with a 5.2-cm cubic trapping cell situated between the poles of a Varian 15-in. electromagnet maintained at 0.9 T. The cell was constructed in our laboratory and includes a 1/4-in.-diameter hole in one of the transmitter plates that permits irradiation with various light sources. High-purity foils of the appropriate metals were attached to the opposite transmitter plate. Metal ions are generated by focusing the beam of a Quanta Ray Nd:YAG laser (frequency doubled to 530 nm) onto the metal foil. Details of the laser ionization technique have been described elsewhere.¹⁰ Generation of gas-phase metal ions in excited states has been reported for both electron impact¹³ and laser desorption.¹⁴ In this study, both Co⁺ and Rh⁺ are believed to be formed exclusively in their ground states since the metal ions react in a first-order manner with no deviations from linearity.

Chemicals were obtained in high purity and used as supplied except for multiple freeze-pump-thaw cycles to remove noncondensable gases. Sample pressures were on the order of 1 × 10⁻⁷ torr. Argon was used as the collision gas for the CID experiments at a total sample pressure of approximately 5 × 10⁻⁶ torr. A Bayard-Alpert ionization gauge was used to monitor pressure.

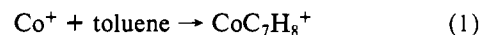
Details of the CID experiments have previously been discussed.^{10,12,15} The collision energy of the ions can be varied (typically between 0 and 100 eV), from which plots of CID product ion intensities vs. kinetic energy can be made. These plots are reproducible to ±5% absolute and are informative, yielding additional structural information. The spread in ion kinetic energies is dependent on the total average kinetic energy and is approximately 35% at 1 eV, 10% at 10 eV, and 5% at

30 eV.¹⁶ H/D exchanges were carried out by using deuterium at a pressure of ~1 × 10⁻⁶ torr. Secondary reactions of the ions undergoing H/D exchanges complicated the interpretation. Addition of the hydrocarbon reactant through a pulsed valve alleviated this problem since no further reaction with the hydrocarbon neutral was observed after a 300-ms interaction time. Hence, the H/D exchanges could then be studied vs. time without loss of the product ions due to competing reactions. Pulsed-valve addition of reagent gases as applied to FTMS has been described in detail.¹⁷

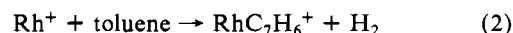
Product intensities listed in Table I are reproducible to ±10% absolute. Laser desorption also produces electron emission from metal surfaces, and some electron-impact ionization of the organic sample can occur in the plasma created by the laser.¹⁸ This process is noticeable for the species studied in this investigation due to their relatively large ionization cross sections. In particular, peaks at *M/z* 91 and 92 were frequently observed. Multiphoton ionization has recently been observed with FTMS.¹⁹ These ions at *M/z* 91 and 92 are not due to multiphoton ionization, however, since the laser beam, defocused from the metal targets, produced no mass 91 and 92 ions. This complication can be entirely circumvented by using swept-double-resonance ejection techniques to quantify the *M/z* 91 and 92 peaks arising from reactions with the metal ions. This was accomplished by trapping the metal ions for 500 ms in the presence of the organic species, isolating the metal ions by swept-double-resonance ejection techniques, and then allowing the metal ions to react with the organic species. Any *M/z* 91 and 92 ions seen in this way must originate from reactions with the metal ions and not from direct laser ionization.

Results and Discussion

Product distributions for the primary reactions of the three polyenes with Co⁺ and Rh⁺ are listed in Table I. Condensation of toluene (reaction 1) is the only process observed for Co⁺.



No direct condensation products were observed for any of the other reactions. Dehydrogenation (reaction 2) is the only



process observed for Rh⁺ reacting with toluene. Toluene, chemisorbed on metal surfaces, has been reported to decompose upon heating to yield hydrogen loss.³⁻⁵ This process is proposed to proceed by initial coordination of the olefin to the

- (11) For a discussion of Fourier transform mass spectrometry, see: (a) Comisarow, M. B.; Marshall, A. G. *Chem. Phys. Lett.* **1974**, *25*, 282. (b) Hunter, R. L.; McIver, R. T., Jr. *Ibid.* **1977**, *49*, 577. (c) Marshall, A. B.; Comisarow, M. B. *J. Chem. Phys.* **1979**, *71*, 4434. (d) Parisod, G.; Comisarow, M. B. *Adv. Mass Spectrom.* **1980**, *8B*, 212.
- (12) (a) Cody, R. B.; Freiser, B. S. *Int. J. Mass Spectrom. Ion Phys.* **1982**, *41*, 99. (b) Cody, R. B.; Burnier, R. C.; Freiser, B. S. *Anal. Chem.* **1982**, *54*, 96.
- (13) (a) Halle, L. F.; Armentrout, P. B.; Beauchamp, J. L. *J. Am. Chem. Soc.* **1981**, *103*, 962. (b) Freas, R. B.; Ridge, D. P. *Ibid.* **1980**, *102*, 7129.
- (14) Kappes, M. M.; Staley, R. H. *J. Phys. Chem.* **1981**, *85*, 942.
- (15) Burnier, R. C.; Cody, R. B.; Freiser, B. S. *J. Am. Chem. Soc.* **1982**, *104*, 7436.

- (16) Huntress, W. T.; Moseman, M. M.; Ellerman, D. D. *J. Chem. Phys.* **1971**, *54*, 843.
- (17) Carlin, T. J.; Freiser, B. S. *Anal. Chem.* **1983**, *55*, 571.
- (18) For a general discussion of laser/metal interactions, see: Ready, J. F. "Effects of High-Power Laser Radiation"; Academic Press: New York, 1971.
- (19) (a) Carlin, T. J.; Freiser, B. S. *Anal. Chem.* **1983**, *55*, 955. (b) Irion, M. P.; Bowers, W. D.; Hunter, R. L.; Rowland, F. S.; McIver, R. T., Jr. *Chem. Phys. Lett.* **1982**, *93*, 375.

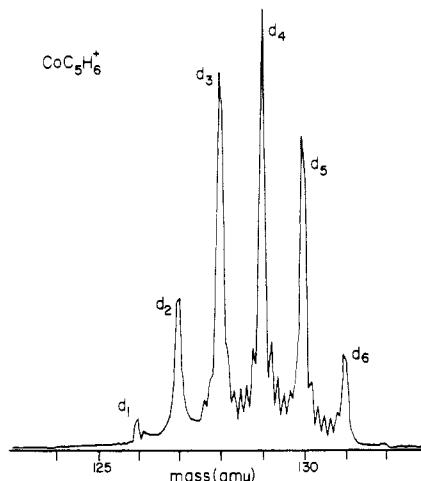
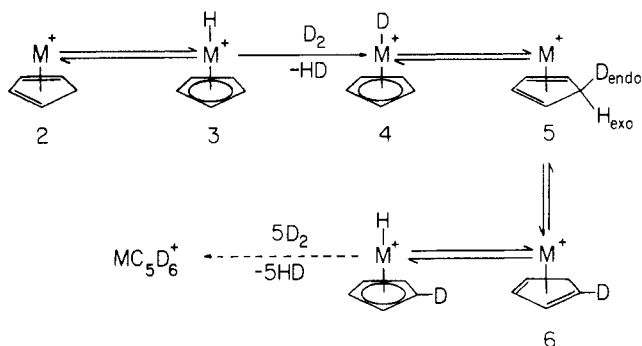
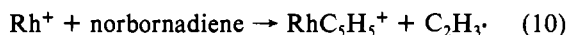


Figure 2. Mass spectrum obtained when $\text{Co-c-C}_5\text{H}_6^+$, generated by reacting Co^+ with norbornadiene (pulsed into the instrument), is trapped in the presence of $\sim 1 \times 10^{-6}$ torr of D_2 for 5 s.

Scheme I



heptatriene. RhC_5H_6^+ probably arises via a retro Diels–Alder reaction followed by loss of acetylene. Again, structural studies are consistent with formation of a $\text{Rh-c-C}_5\text{H}_6^+$ complex. In addition, RhC_5H_5^+ is also observed and may be generated either by loss of acetylene followed by H• loss or by direct loss of $\text{C}_2\text{H}_3\cdot$ (reactions 9 and 10). Assuming that the product



of reactions 9 and 10 is cyclopentadienyl bound to Rh^+ , then process 9 requires $D^\circ(\text{Rh}^+-\text{c-C}_5\text{H}_5) > 111$ kcal/mol to be exothermic while process 10 requires $D^\circ(\text{Rh}^+-\text{c-C}_5\text{H}_5) > 77$ kcal/mol to be exothermic.²⁰ A bond strength of 111 kcal/mol for cyclopentadienyl seems high; hence, process 9 is believed to be responsible for formation of $\text{Rh-c-C}_5\text{H}_5^+$.

Co^+ reacts with norbornadiene to produce predominantly CoC_5H_6^+ and CoC_2H_2^+ ions. Again, these products can be envisioned as proceeding by a retro Diels–Alder process followed by competitive loss of either cyclopentadiene or acetylene. A small amount of CoCH_2^+ and CoC_6H_6^+ is also observed.

$\text{Co-c-C}_5\text{H}_6^+$, generated from either cycloheptatriene or norbornadiene, undergoes six H/D exchanges in the presence of excess deuterium. Figure 2 shows the spectrum obtained when CoC_5H_6^+ , produced from norbornadiene, is trapped in the presence of about 1×10^{-6} torr of D_2 . The initial exchange is rapid with the remaining five exchanges occurring considerably more slowly ($\sim 1/10$ th the rate of the first). A mechanism for the H/D exchange is shown in Scheme I and involves a rapid equilibrium between the cyclopentadiene (**2**) and hydridocyclopentadienyl (**3**) structures. Oxidative addition of D_2 to **3** is followed by reductive elimination of HD, forming **4**. Although complexes **4** and **5** are in rapid equilibrium, the

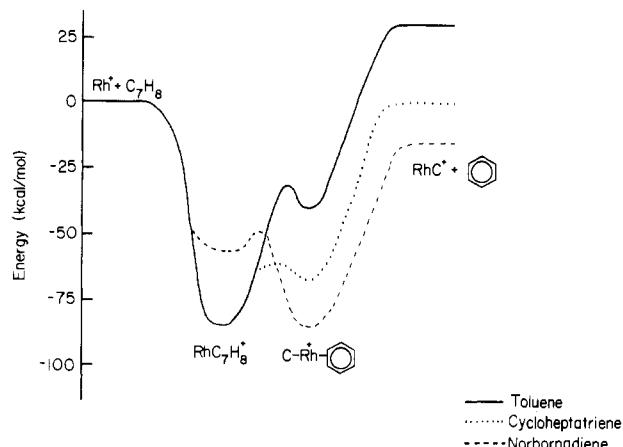


Figure 3. Potential energy surface for RhC^+ formation from toluene, cycloheptatriene, and norbornadiene.

incorporated deuterium will remain unscrambled in the endo position. Complex **5** rearranges to **6** via a [1,5] sigmatropic shift (thermally allowed in the ground state²³), which is known to occur rapidly at room temperature in labeled cyclopentadiene,²⁴ permitting the remaining hydrogens to be exchangeable. This mechanism then accounts for the observed H/D exchanges for $\text{Co-c-C}_5\text{H}_6^+$. In a similar gas-phase experiment, MCp^+ ($\text{M} = \text{Fe}, \text{Co},$ or Ni ; $\text{Cp} =$ cyclopentadienyl) ions were shown to undergo only four alkylations of the ring by methyl bromide and an interconversion of the structures analogous to **2** and **3** in Scheme I was postulated.²⁵

No H/D exchanges were seen for the $\text{Rh-c-C}_5\text{H}_6^+$ ions with deuterium. This result is consistent with a previous study in which $\text{Rh-c-C}_5\text{H}_6^+$, formed from cyclopentane, also failed to undergo any H/D exchanges.²⁶ Interestingly, this same study revealed that RhC_5H_6^+ , formed from reaction of Rh^+ with propane, undergoes five H/D exchanges with deuterium while CoC_5H_6^+ formed in a similar fashion does not exchange any hydrogens with deuterium.^{10d} A $\text{CpRhC}_3\text{H}_5^+$ complex has been reported to undergo four H/D exchanges on the allyl ligand with excess D_2 .²⁷ These results indicate that $\text{Rh-c-C}_5\text{H}_6^+$ may be frozen in a cyclopentadiene structure.

The differences in the fractions of RhC_7H_6^+ and RhC^+ formation for the three C_7H_8 isomers may be explained by considering the potential energy surface shown in Figure 3. This diagram has been simplified by omitting the intermediates leading to formation of the carbide–benzene species. Initially, the cyclic polyenes interact with Rh^+ , forming complexes activated by the strength of the metal–ligand bond energy. Dehydrogenation occurs producing RhC_7H_6^+ ions, which ultimately rearrange to a carbide–benzene structure (**1**) upon activation. Assuming $D^\circ(\text{Rh}^+-\text{C}) \sim 148$ kcal/mol and $D^\circ(\text{Rh}^+-\text{benzene}) \sim 71$ kcal/mol, then formation of structure **1** is 40 kcal/mol exothermic for toluene, 71 kcal/mol exothermic for cycloheptatriene, and 86 kcal/mol exothermic for norbornadiene.²⁰ For toluene, loss of benzene from **1** would be endothermic by 31 kcal/mol. Consistent with this assertion is the fact that RhC_7H_6^+ is the only primary reaction product observed for toluene. Absence of the formation of RhC^+ for toluene then implies an upper limit of 179 kcal/mol for $D^\circ(\text{Rh}^+-\text{C})$; $D^\circ(\text{Rh}^+-\text{C}) = 163.5 \pm 16$ kcal/mol. The

(23) Spangler, C. W. *Chem. Rev.* **1976**, *76*, 187.

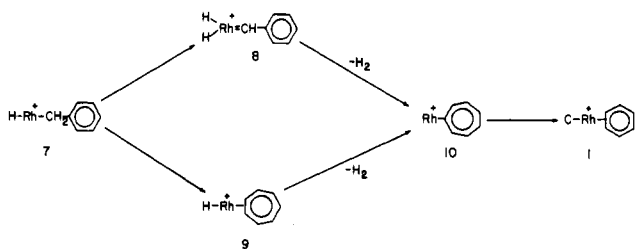
(24) (a) Roth, W. *Tetrahedron Lett.* **1964**, 1009. (b) Berson, J. A.; Aspelin, G. G. *Tetrahedron* **1964**, *20*, 2697.

(25) (a) Corderman, R. R.; Beauchamp, J. L. *Inorg. Chem.* **1978**, *17*, 68. (b) Jones, R. W.; Staley, R. H. *Int. J. Mass Spectrom. Ion Phys.* **1981**, *39*, 35.

(26) Byrd, G. D.; Freiser, B. S. *J. Am. Chem. Soc.* **1982**, *104*, 5944.

(27) Beauchamp, J. L.; Stevens, A. E.; Corderman, R. R. *Pure Appl. Chem.* **1979**, *51*, 967.

Scheme II



$\text{RhC}^+:\text{RhC}_7\text{H}_6^+$ ratio is greater for norbornadiene than for cycloheptatriene, as predicted in Figure 3, since formation of 1 is 15 kcal/mol more exothermic for norbornadiene than for cycloheptatriene.

A proposed mechanism for dehydrogenation and carbide-benzene formation is outlined in Scheme II for toluene. Initially, Rh^+ oxidatively adds to an aliphatic C-H bond,²⁸ generating a hydrido-benzyl complex (7). This is followed by an α -hydride abstraction, producing a dihydride-phenyl-carbene complex (8), which reductively eliminates hydrogen with rearrangement to a σ -bound $\text{c-C}_7\text{H}_6$ complex (10). In addition, the benzyl group in complex 7 can rearrange to tropylium,²⁹ forming 9. Hydride abstraction by 9 followed by dehydrogenation results in formation of 10. Complex 10 then rearranges to the carbide-benzene complex 1. In ad-

dition, complex 8, after dehydrogenation, may rearrange directly to the carbide-benzene structure. Both dehydrogenation pathways are required to account for the deuterium losses observed for toluene- $\alpha,\alpha,\alpha\text{-d}_3$. In addition, the carbide-benzene formation process for all three C_7H_8 isomers may proceed through a common intermediate, probably the σ -bound $\text{c-C}_7\text{H}_6$ species (10).

Conclusions

In general, Rh^+ is more reactive toward these cyclic polyenes than Co^+ . This is in accord with a previous study on the reactions of Rh^+ with alkanes.²⁶ Dehydrogenation of the three cyclic polyenes is unique for Rh^+ . Structural studies indicate that the dehydrogenation product, RhC_7H_6^+ , rearranges upon activation to a common intermediate for all three C_7H_8 isomers, presumably a carbide-benzene complex (1). This process is related to that reported for the surface chemistry of cycloheptatriene and norbornadiene.⁶ On metal surfaces several metal centers may be involved in the dehydrogenation and benzene formation processes. However, in the gas phase, only one metal center is involved. The exact mechanism for the dehydrogenation process in the gas phase is unclear, however, and future studies call for the use of labeled compounds to help delineate this mechanism as well as the mechanisms involved for the C-C bond cleavage products observed for both metal ions.

Acknowledgment is made to the Division of Chemical Sciences, Office of Basic Energy Sciences, U.S. Department of Energy (Grant DE-AC02-80ER10689), for supporting this research and the National Science Foundation (Grant CHE-8002685) for providing funds to purchase the FT mass spectrometer.

Registry No. C_7H_8 , 108-88-3; Co^+ , 16610-75-6; Rh^+ , 20561-59-5; $\text{c-C}_7\text{H}_6$, 544-25-2; toluene- $\alpha,\alpha,\alpha\text{-d}_3$, 1124-18-1; norbornadiene, 121-46-0.

(28) Evidence against initial insertion into an aromatic C-H bond is that Rh^+ reacts with benzene to generate the condensation product RhC_6H_6^+ exclusively with no dehydrogenation observed.

(29) Rearrangement of benzyl ions to tropylium ions has been observed in the gas phase; see for examples: (a) Jackson, J. A.; Lias, S. G.; Ausloos, P. *J. Am. Chem. Soc.* **1977**, *99*, 7515. (b) Kuck, D.; Grutzmacher, H.-F. *Org. Mass Spectrom.* **1979**, *14*, 86. (c) McLouglin, R. G.; Morrison, J. D.; Traeger, J. C. *Ibid.* **1979**, *14*, 014. (d) McLafferty, F. W.; Bockhoff, F. M. *J. Am. Chem. Soc.* **1979**, *101*, 1783. (e) Cone, C.; Dewar, M. J. S.; Landman, D. *Ibid.* **1977**, *99*, 372.

Contribution from Chemistry Department A,
The Technical University of Denmark, DK-2800 Lyngby, Denmark

Phase Diagram of the NaCl-AlCl_3 System near Equimolar Composition, with Determination of the Cryoscopic Constant, the Enthalpy of Melting, and Oxide Contaminations

ROLF W. BERG,* HANS AAGE HJULER, and NIELS J. BJERRUM*

Received March 10, 1983

The phase diagram of the NaCl-AlCl_3 system near the equimolar composition is reported with high precision. The freezing point of the pure, congruently melting compound NaAlCl_4 was determined to be 156.7 ± 0.1 °C. The molal freezing point depression constant of equimolar NaCl-AlCl_3 melts was estimated to be 19 ± 2 °C kg mol⁻¹. The overall enthalpy of melting for NaAlCl_4 given in recent literature can be divided into two parts, a premelting part ($\Delta H_p \approx 4.5$ kJ mol⁻¹), whose origin is discussed, and a real melting part ($\Delta H_f \approx 15.5$ kJ mol⁻¹). Oxide impurities were always found to be present in these melts. The influence of oxides, their origin, and their determination were considered, as were phase diagram corrections for the presence of oxide impurities. The freezing point depressions caused by added AlOCl showed the most likely constitution of the dissolved oxide to be $(\text{AlOCl})_2 \cdot \text{AlCl}_4^-$ in equilibrium with other species.

Introduction

Chloroaluminate melts have attracted considerable interest as high-temperature ionic solvents with low crystallization temperatures. These properties have led to applications in, e.g., the ALCOA chloride process for producing aluminum via AlCl_3 ,¹ as reaction media, and, possibly, in rechargeable

high-energy-density batteries.

Considering the importance of the NaCl-AlCl_3 system within these respects, it is surprising to note that neither the freezing (or melting) point of the pure NaAlCl_4 compound nor the NaCl-AlCl_3 phase diagram in the vicinity of the equimolar mixture is accurately known. In addition to this, the freezing point depression (cryoscopic) constant for NaAlCl_4 is unknown.

The present work was started in order to compensate for these shortcomings. Detailed measurement of the phase di-

(1) Grjotheim, K.; Krohn, C.; Øye, H. A. *Aluminum (Düsseldorf)* **1975**, *51*, 697.